IN SILICO STUDY: SECONDARY METABOLITES FROM RED GINGER RHIZOME (*Zingiber Officinale* Var. Rubrum) AS POTENTIAL INHIBITORS OF3CLpro AND PLpro OF SARS-CoV-2

Meilia Suherman[1], Selvira Anandia Intan Maulidya[1*]
[1]*Department of Pharmaceutical Analysis and Medicinal Chemistry, Faculty of Mathematics and Natural Sciences, Universitas Garut, West Java – Indonesia*
Jl. Jati 42B, Jati, Tarogong Kaler, Garut
[*]Email Corresponding: selvira@uniga.ac.id

ABSTRACT

The COVID-19 outbreak prompted the development of novel drugs to treat the disease. Targeting of virus proteins has attracted great interest in the discovery of COVID-19 drugs. 3CLpro and PLpro are promising targets because of their important role in viral replication. Hence, various efforts have been made to find specific therapeutics for COVID-19, including those derived from plants as anti-Covid-19. Red ginger rhizome (Zingiber officinale var. rubrum) contains secondary metabolites that are known for their health benefits. This in silico study aimed to determine the potency of red ginger rhizome as PLpro and 3CLpro of SARS-CoV-2 inhibitor which may be applied to treat COVID-19. This research was conducted using molecular docking and molecular dynamics simulations. The molecular docking simulation of red ginger compounds in complex with SARS-CoV-2 PLpro showed that 27 compounds have a binding free energy (ΔG) lower than that of the reference ligand. On the other hand, none of the complexes between red ginger compounds and 3CLpro had a lower binding free energy than the reference ligand. Visualization of interaction features at the PLpro of SARS-CoV-2's active site shows that secondary metabolites dominantly interact with hydrogen bonds. The ar-curcumene and PLpro complex of SARS-CoV-2 appears very stable and has the lowest flexibility compared to HBA as a native ligand and molnupiravir as a reference ligand based on RMSD and RMSF plot analysis using molecular dynamic simulation. This in silico study concluded that one of the red ginger rhizome secondary metabolites, ar-curcumene, has potential as a PLpro of SARS-CoV-2 inhibitor. Furthermore, it could be optimized and developed as a candidate drug for COVID-19 treatment.
Keywords: red ginger rhizome, SARS-CoV-2, 3CLpro, PLpro

INTRODUCTION

Currently, the world's attention is focused on the coronavirus disease (COVID-19), which is caused by the SARS-CoV-2 virus. COVID-19 has emerged as the most dangerous pandemic of the twentieth century, infecting over 600 million people and causing over six million fatalities worldwide as of January 2023. In September 2021, Indonesia reported more than 6 million confirmed cases and 161,000 deaths from confirmed coronavirus. As a result, several measures, including drug research and development, have been attempted to aid in the spread of COVID-19. Furthermore, significant efforts have been made to develop new rational drugs against COVID-19 that target non-structural proteins, spiked proteins, RNA-dependent RNA polymerase (RdRp), and angiotensin-converting enzyme II (ACE2) (Abdelli *et al.*, 2021)(Babadaei *et al.*, 2020)(Basit, Ali and Rehman, 2021)(Hasan *et al.*, 2021)(Sinha *et al.*, 2021)(Suharyani *et al.*, 2021) . Because the selection of targets in the form of specific enzymes is often the primary drug target as an antiviral, coronavirus-specific enzymes may be potential targets for treating COVID-19. The key targets for COVID-19 drug

development are 3CLpro (3-Chymotrypsin-Like Protease) and PLpro (Papain-Like Protease). Proteases are essential for viral replication. 3CLpro is encoded by the coronavirus RNA and is essential for viral particle growth. (Needle, Lountos and Waugh, 2015). On the other hand, the active site of papain-like protease (PLpro) consists of a catalytic triad (Cys111, His272 and Asp286). Furthermore, its primary function is to convert viral polypeptides into functional proteins, which then deubiquitinize and inhibit the host's antiviral reactions by hijacking the ubiquitin (Ub) enzyme, which is essential for the host's defense mechanism (Amin et al., 2009).

Herbal medicines are currently in high demand for basic healthcare in industrialized countries because of their efficacy, safety, and lack of adverse effects (Bhargava et al., 2012). According to World Health Organization research, 80% of the population in underdeveloped nations relies on jamu for primary health care, with plants accounting for 85% of jamu (Ghasemzadeh Jaafar and Rahmat, 2015).The rhizomes of Zingiber officinale var. Rubrum has long been used in Indonesian herbal medicine. Many studies have confirmed the anti-inflammatory (Fikri et al., 2016), antioxidant (Sholikhati et al., 2022), antiemetic (Hartati et al., 2022), antibacterial (Assegaf et al., 2020), and antidiabetic (Eliza Arman, 2016) properties of red ginger.

Various new drug developments, including the in silico method, are being used to accelerate the discovery of anti-COVID-19 drugs, because they are supported by good computational techniques and also shorten the time in the drug discovery process, in silico methods for developing new drugs are growing rapidly. Based on previous research, an experiment was developed to identify anti-COVID-19 candidates by studying polyphenol chemicals in green tea using in silico methodologies. Therefore, it can be utilized as a first-line treatment for COVID-19, particularly in Indonesia.

RESEARCH METHODS
Tools And Materials

44 structures of secondary metabolites of red ginger rhizome were obtained from the site https://pubchem.ncbi.nlm.nih.gov. The 3CLpro SARS-CoV2 receptors (PDB ID 7SI9) and PLpro (PDB ID 7OFT) were downloaded from the https://rcsb.org site in PDB format. Hardware: ASUS A456U notebook (operating system: Microsoft Windows 10 Pro and Ubuntu 17.04), 64-bit; memory:4GB; Processor: Intel Core i5-7200U, Personal Computer (operating system: Ubuntu 16.04 LTS, Xeon Processor, 16 GB Memory). Software: Discovery Studio Visualizer®, MarvinSketch Version 17.2.13®, Autodock Tools®, Autodock Vina®, YASARA®, Open Babel GUI®, KNApSAck (http://www.knapsackfamily.com/KNApSAcK/), PASS (Prediction of Activity Spectra for Substances) Online (http://way2drug.com/passonline/predict.php), STITCH (http://stitch.embl.de/), PreADMET (http://preadmet.bmdrc.org/) , PubChem (http://pubchem.ncbi.nlm.nih.gov), google colab, google drive, CHEMAIRS (https://chemairs.chemicalai.cn/#/), Lipinski's Rule of Five (http://www .scfbio-iitd.res.in/software/drugdesign/lipinski.jsp), and the Protein Data Bank (PDB) (https://www.rscb.org/).

Research Procedure
1. **Coumpound library selection and ligand preparation**

   The compound of red ginger rhizome obtained through various library sources and based on search results using the KNApSAcK online database site (http://www.knapsackfamily.com/KNApSAcK/)
2. **Geometry Optimization**

   The shape of the 3D molecular structure of the secondary metabolites contained in red ginger rhizomes was determined by geometric optimization using MarvinSketch with the semi-empirical AM1 method.

3. **Lipinski's Rule of Five Testing**

In this study, the ligands or molecules evaluated were the secondary metabolites of the ginger rhizome. Ligands were redrawn in ChemDraw® Ultra 12.0 and energy was minimized in Chem3D® Pro 12.0 before being stored in.pdb format. Following preparation, the physicochemical properties of the compounds were determined using Lipinski's Rule of Five.

4. **Pre-ADMET Evaluation**

The tests were conducted to examine the first characteristics of pharmacokinetics, such as absorption and distribution, as well as toxicity testing, such as the mutagenic and carcinogenic qualities of the substances. Testing is done out using a specific program that is carried out online on the http://preadme.bmdrc.kr/ site. After drawing the structure of the test substance, a click was submitted for the analysis. The collected results are data in.pdb format.

5. **Protein Selection and Preparation**

Receptors downloaded via PDB website (https://www.rscb.org/) with PDB ID 7SI9 for main protease (3CLpro) and PDB ID 7OFT for papain like protease (PLpro), receptor-ligand complex separated and prepared using Autodock Vina® software, then validated

6. **Molecular Docking**

The docking algorithm was validated by redoxing natural ligands on the SARS-CoV2 3CLpro and PLpro receptors. Molecular docking was performed using the previously validated parameters. Canonical SMILES of the test compound were obtained from the Pubchem website (http://pubchem.ncbi.nlm.nih.gov) then the optimization process was carried out, then the docking process was carried out using Autodock Vina® software and visualization was carried out using the Discovery Studio Visualizer software®. The improved 3D-ligand structures were then bound to the active sites of 3CLpro and PLpro. The binding energy (G), inhibition constant, and interaction pose were calculated from these results. Ligands with the best docking results moved on to the next round of testing, which was a molecular dynamics simulation.

7. **Molecular Dynamics Simulation**

Molecular dynamics simulations were performed using open MM software on the complex between 3CLpro and PLpro SARS-CoV2 and the ligand with the lowest binding energy based on molecular docking experiments. Begin created a protein and ligand topology. The ff19SB force field was used to add the ligand topology, and the GAFF2 force field with the TIP3P water model was used to add the receptor topology for 10 ns.

RESULTS AND DISCUSSION

1. **Geometry Optimization**

The active compounds in ginger (*Zingiber Officinale* Var. Rubrum) was discovered using multiple literature sources and based on search results obtained using the online database site KNApSAcK, which yielded 44 secondary metabolites that were detected in red ginger rhizomes. Geometric optimization of the 3D molecular structure of the secondary compounds found in red ginger rhizomes was performed using MarvinSketch and the semi-empirical AM1 method. Furthermore, using OpenBabel software, the structure was optimized and saved in pdb format.

2. *Lipinski's Rule of Five*

Lipophilicity (CLogP) less than 5, number of hydrogen bond donors less than 5, number of hydrogen bond acceptors less than 10, and molecular weight (BM) less than 500 g/mol are physicochemical parameters related to the permeability for passive diffusion determined by Lipinski's Rule of Five. The majority of the 44 compounds tested met Lipinski's Rule of Five requirements, but three compounds, notably 10-

shogaol, gingerdione, and a-Humulene, did not match Lipinski's standards in terms of lipophilicity.

Table I. Druglikeness Prediction Results of Test Compounds Based on Lipinski's Rule of Five

No.	Compound	MW (g/mol)	Log P	H Donor	H acceptor
1	6-gingerol	294	3.23	2	4
2	8-gingerol	322	4.01	2	4
3	10-gingerol	350	4.79	2	4
4	6-shogaol	276	4.03	1	3
5	8-shogaol	304	4.81	1	3
6	10-shogaol	332	5.59	1	3
7	Zingerone	194	1.92	1	3
8	1-dehydro-6-gingerdione	290	5.52	1	4
9	a-Pinene	136	2.99	0	0
10	Camphene	136	2.99	0	0
11	b-Pinene	136	2.99	0	0
12	6-Methyl-5-hepten-2-one	126	2.32	0	1
13	Myrcene	134	3.47	0	0
14	Limonene	136	3.3	0	0
15	1,8-Cineole	154	2.74	0	1
16	2-Heptyl acetate	158	2.51	0	2
17	Terpinolene	136	3.45	0	0
18	Linalool	154	2.66	1	1
19	Camphor	152	2.4	0	1
20	Camphene hydrate	154	2.19	1	1
21	Citronellal	154	2.95	0	1
22	Isoborneol	154	2.19	1	1
23	Borneol	154	2.19	1	1
24	a-Terpineol	154	2.5	1	1
25	Myrtenal	150	2.17	0	1
26	b-Citronellol	156	2.75	1	1
27	Neral	152	2.87	0	1
28	Geraniol	154	2.67	1	1
29	geranial	152	2.87	0	1
30	Bornyl acetate	196	2.76	0	2
31	Myrtenyl acetate	196	2.76	0	2
32	Neryl acetate	196	3.24	0	2
33	Geranyl acetate	196	3.24	0	2
34	b-Elemene	204	4.74	0	0
35	b-Caryophyllene	204	4.72	0	0
36	a-Humulene	204	5.03	0	0
37	Allo-aromadendrene	204	4.27	0	0
38	ar-curcumene	202	4.84	0	0
39	a-Zingiberene	204	4.89	0	0
40	a-Selinene	204	4.72	0	0
41	b-Sesquiphellandrene	204	4.89	0	0
42	a-Elemol	222	3.94	1	1
43	Caryophyllene oxide	220	3.93	0	1
44	a-Bisabolol	222	4.23	1	1

3. Absorption, Distribution and Toxicity Test

Absorption, distribution, and toxicity parameters were measured using a tool available online at https://preadmet.bmdrc.kr/adme/. The chemical structure of the substance was sketched and sent to the site, and the application automatically calculated the expected value. Cell permeability of human colon adenocarcinoma (Caco-2), Human Intestinal Absorption (HIA), and Plasma Protein Binding (PPB) were the criteria used. The ability of the drug to be absorbed in the intestine (Human Intestinal Absorption) and the permeability of Caco-2 cells were used to predict the drug absorption.

Table II. Prediction Results of Pharmacokinetic Profiles and Toxicity of Test Compounds Based on Pre-ADMET

| No | Compound | Absorption | | Distribution |
		HIA (%)	Caco-2 Cell (nm sec)	Plasma Protein Binding (%)
1	6-gingerol	91.96	24.52	100
2	8-gingerol	92.52	31.11	100
3	10-gingerol	92.96	39.67	100
4	6-shogaol	95.18	51.86	100
5	8-shogaol	95.34	54.53	100
6	10-shogaol	95.52	55.89	100
7	Zingerone	94.25	29.05	79
8	1-dehydro-6-gingerdione	95.78	29.49	93.05
9	Camphene	100	23.49	100
10	alpha-Pinene	100	23.63	100
11	b-Pinene	100	23.49	100
12	6-Methyl-5-hepten-2-one	100	54.04	37.79
13	Myrcene	100	23.63	100
14	Limonene	100	23.63	100
15	1,8-Cineole	100	21.89	100
16	2-Heptyl acetate	100	26.19	100
17	Terpinolene	100	23.63	93.16
18	Linalool	100	29.36	100
19	Camphor	100	26.82	100
20	Camphene hydrate	100	40.48	100
21	Citronellal	100	13.73	100
22	Isoborneol	100	24.23	100
23	Borneol	100	24.23	100
24	a-Terpineol	100	50.81	23.42
25	Myrtenal	100	22.04	49.76
26	b-Citronellol	100	8.91	100
27	Neral	100	13.97	100
28	Geraniol	100	8.76	100
29	geranial	100	13.97	100
30	Bornyl acetate	100	37.68	83.33
31	Myrtenyl acetate	100	30.92	79.33
32	Neryl acetate	100	44.51	100
33	Geranyl acetate	100	44.51	100
34	b-Elemene	100	23.49	100
35	b-Caryophyllene	100	23.63	100
36	a-Humulene	100	23.63	100
37	Allo-aromadendrene	100	23.49	100

No	Compound	Absorption		Distribution
		HIA (%)	Caco-2 Cell (nm sec)	Plasma Protein Binding (%)
38	ar-curcumene	100	23,40	100
39	a-Zingiberene	100	23,40	100
40	a-Selinene	100	23.63	100
41	b-Sesquiphellandrene	100	23,40	100
42	a-Elemol	100	55.32	99.19
43	Caryophyllene oxide	100	56.35	90.85
44	a-Bisabolol	100	51.1	90.29

Information:

HIA (%):	Caco-2 (nm sec):	PPB (%):
70-100 is well absorbed	>70 high permeability	>90 tightly bound
20-70 absorbed enough	4-70 medium permeability	<90 weakly bound
<20 poorly adsorbed	<4 low permeability	

HIA refers to the process by which orally administered drugs are absorbed from the gastrointestinal system into the bloodstream of the body (Cheng et al., 2012). A higher value indicated that the compound had a higher probability of being absorbed into the bloodstream. The 44 compounds were predicted to be well absorbed when administered orally, with a high HIA value.

Caco-2 refers to human colon epithelial cancer cells, which are used as a model for human intestinal absorption of drugs. These cells are used because, when cultured, they form tight junctions between cells, which makes them resemble the paracellular movement of compounds across the monolayer. Additionally, Caco-2 cells are known to express transporter proteins, efflux proteins, and conjugation enzymes, which are common pathways for the transcellular entry and metabolic transformation of external substances. Hence, Caco-2 permeability is an indirect measure of human intestinal absorption (Cheng et al., 2012).

A compound needs to bind with plasma protein so that it can be dissociated by the bloodstream to reach its target (drug receptor/enzymes/etc). Drug efficiency may be affected by the degree to which the drug binds to proteins within the body. The less bound a drug, the more efficiently it can be distributed. Plasma protein binding (PPB) strongly affects drug distribution and pharmacokinetic behavior, resulting in an overall pharmacological action. Extended plasma protein binding may be associated with drug safety issues and adverse effects (Lambrinidis Vallianatou and Tsantili-Kakoulidou, 2015).

Table III. Prediction Results of Toxicity Profiles of Test Compounds Based on Pre-ADMET

No	Compound	Cramer Rules	Kroes TTC	Carcinogenicity	Mutagenicity (*Ames Test*)
1	6-gingerol	2	1	8;9	2
2	8-gingerol	2	1	8;9	2
3	10-gingerol	2	1	8;9	2
4	6-shogaol	2	2	1;9	1
5	8-shogaol	2	1	8;9	2
6	10-shogaol	2	1	8;9	2
7	Zingerone	1	1	8;9	2
8	1-dehydro-6-gingerdione	2	1	8;9	2
9	a-Pinene	1	1	8;9	2
10	Camphene	1	1	8;9	2

No	Compound	Cramer Rules	Kroes TTC	Carcinogenicity	Mutagenicity (*Ames Test*)
11	b-Pinene	1	1	8;9	2
12	6-Methyl-5-hepten-2-one	1	1	8;9	2
13	Myrcene	1	1	8;9	2
14	Limonene	1	1	8;9	2
15	1,8-Cineole	3	1	2;8	2
16	2-Heptyl acetate	1	1	8;9	2
17	Terpinolene	1	1	8;9	2
18	Linalool	3	1	8;9	2
19	Camphor	3	1	8;9	2
20	Camphene hydrate	3	1	8;9	2
21	Citronellal	1	2	1;9	1
22	Isoborneol	1	1	8;9	2
23	Borneol	1	1	8;9	2
24	a-Terpineol	3	1	8;9	2
25	Myrtenal	3	2	1;4;9	1;4
26	b-Citronellol	1	1	8;9	2
27	Neral	1	1	4;8;9	2;4
28	Geraniol	1	1	8;9	2
29	geranial	1	1	4;8;9	2;4
30	Bornyl acetate	1	1	8;9	2
31	Myrtenyl acetate	1	1	8;9	2
32	Neryl acetate	1	1	8;9	2
33	Geranyl acetate	1	1	8;9	2
34	b-Elemene	1	1	8;9	2
35	b-Caryophyllene	1	1	8;9	2
36	a-Humulene	1	1	8;9	2
37	Allo-aromadendrene	1	1	8;9	2
38	ar-curcumene	2	1	8;9	2
39	a-Zingiberene	1	1	8;9	2
40	a-Selinene	1	1	8;9	2
41	b-Sesquiphellandrene	1	1	8;9	2
42	a-Elemol	3	1	8;9	2
43	Caryophyllene oxide	1	2	1;9	1
44	a-Bisabolol	3	1	8;9	2

Information:
Cramer rules:
1 = low (Class I),
2 = intermediate (Class II),
3 = high (Class III).
Kroes TTC decision tree:
1 = Subtance would not be expected to be a safety concern;
2 = Negligible risk (low probability of lifetime cancer risk greater than 1 in 10^6)
3 = Risk assesment requires compound-specific toxicity data.
Carcinogenicity:
1 = Structural alert for genotoxic carcinogenicity;
2 = Structural alert for nongenotoxic carcinogenicity;
8 = Negative for genotoxic carcinogenicity;
9 = Negative for non-genotoxic carcinogenicity
Mutagenicity:
1 = Structural alert for S. typhimurium mutagenicity;
2 = No alert for S. typhimurium mutagenicity;
4 = Unlikely to be a S. typhimurium TA100 mutagen based on QSAR

The PreADMET software was used to predict the toxicity of the compounds. The Cramer Rules were used to predict the toxicity level based on the functional group; the Kroes TTC was used to predict the safety limits of the compounds, and the carcinogenicity and mutagenicity tests were used to determine whether the test compound had carcinogenic and mutagenic effects. The Cramer rules test yielded 28 compounds in class I, 8 compounds in class II, 8 compounds in class III. Based on the Kroes TTC test, 40 compounds were predicted to be safe, and only 4 compounds had negligible risk. Lastly, Pre-ADMET predicted 7 compounds had a structural alert for carcinogenicity and 4 compounds had a structural alert for mutagenicity.

4. Molecular Docking

Molecular docking was performed against the main protease receptor (3CLpro) (PDB ID: 7SI9) (**Figure 1**) and the papain-like protease receptor (PLpro) (PDB ID 7OFT) (**Figure 2**). Molecular docking of red ginger compounds in complex with PLpro SARS-CoV-2 showed that 27 compounds had a bond free energy (ΔG) lower than the original ligand, 4 compounds had a bond free energy (ΔG) lower than the reference ligand (molnupiravir), and ar-curkumen showed the lowest bond free energy value compared to the other compounds (**Table IV**). On the other hand, none of the complexes between the red ginger compound and 3CLpro had a lower bond free energy than the reference ligand (**Table V**). Molecular docking between ar curcumene and PLpro from SARS-CoV-2 indicated the presence of van der Waals interaction residues around the cavities (Pro77, Tyr74, and Tyr75) at the catalytic site (**Figure 3**).
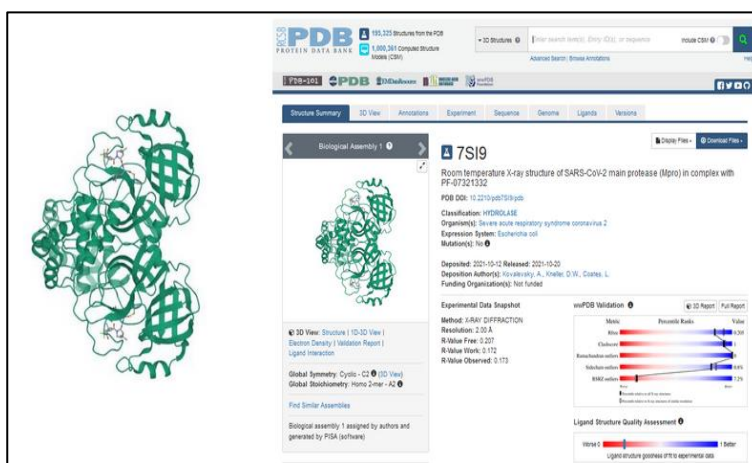
Figure 1. 3D structure of the 3CLpro receptor PDB ID 7SI9
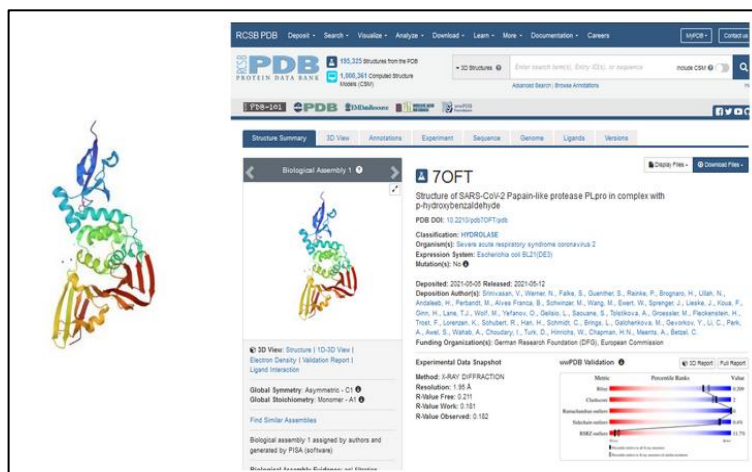
**Figure 2. 3D structure of papain like protease receptor (PLpro) PDB ID 7OFT**

Table IV. **Molecular binding of the active compound of red ginger rhizome (Zingiber officinale var. Rubrum) against 3CLpro receptor**

No.	Compound	ΔG (KCal/mol)
1	Native ligand	-8.3
2	1-dehydro-6-gingerdione	-6.2
3	8-gingerol	-6
4	6-shogaol	-6
5	8-shogaol	-5.9
6	6-gingerol	-5.8
7	Allo-aromadendrene	-5.8
8	a-Elemol	-5.8
9	b-Caryophyllene	-5.7
10	Caryophyllene oxide	-5.7
11	a-Bisabolol	-5.7
12	10-gingerol	-5.6
13	a-Selinene	-5.6
14	b-Elemene	-5.5
15	a-Humulene	-5.4
16	10-shogaol	-5.3
17	Myrtenyl acetate	-5.3
18	b-Sesquiphellandrene	-5.3
19	Geranyl acetate	-5.1
20	ar-curcumene	-5.1
21	Zingerone	-5.1
22	Neryl acetate	-5
23	Myrtenal	-4.9
24	a-Terpineol	-4.8
25	Bornyl acetate	-4.8
26	Isoborneol	-4.7
27	a-Pinene	-4.6
28	1,8-Cineole	-4.6
29	Linalool	-4.6
30	Camphene hydrate	-4.6
31	Camphene	-4.5
32	b-Pinene	-4.5
33	Limonene	-4.5
34	Terpinolene	-4.5
35	Camphor	-4.5
36	Citronellal	-4.5
37	Borneol	-4.5
38	b-Citronellol	-4.5
39	Geraniol	-4.5
40	geranial	-4.5
41	a-Zingiberene	-4.5
42	2-Heptyl acetate	-4.2
43	Neral	-4.2
44	6-Methyl-5-hepten-2-one	-4.1
45	Myrcene	-4.1

Table V. **Molecular binding of the active compound of red ginger rhizome (Zingiber officinale var. Rubrum) to the PLpro receptor**

No.	Compound	ΔG (KCal/ mol)
1	Native ligand	-6.1
2	Molnupiravir	-7.2
3	**ar-curcumene**	**-8.5**
4	**a-Zingiberene**	**-8.4**
5	**b-Sesquiphellandrene**	**-8.4**
6	**Zingerone**	**-7.3**
7	a-Terpineol	-7.1
8	Myrtenyl acetate	-7.1
9	Terpinolene	-7.1
10	b-Caryophyllene	-7
11	6-shogaol	-6.9
12	Neryl acetate	-6.9
13	a-Selinene	-6.8
14	b-Citronellol	-6.8
15	b-Elemene	-6.8
16	Geranyl acetate	-6.8
17	Limonene	-6.8
18	Linalool	-6.8
19	a-Pinene	-6.7
20	Geraniol	-6.7
21	b-Pinene	-6.5
22	Camphene	-6.5
23	Citronellal	-6.5
24	geranial	-6.5
25	Myrtenal	-6.5
26	Neral	-6.5
27	Myrcene	-6.3
28	6-Methyl-5-hepten-2-one	-6.1
29	1-dehydro-6-gingerdione	-6
30	6-gingerol	-6
31	2-Heptyl acetate	-5.9
32	8-shogaol	-5.7
33	Camphene hydrate	-5.7
34	1,8-Cineole	-5.6
35	10-gingerol	-5.5
36	a-Humulene	-5.3
37	Borneol	-5.3
38	Camphor	-5.3
39	Bornyl acetate	-5.2
40	8-gingerol	-5
41	Isoborneol	-4.9
42	10-shogaol	-4.8
43	Allo-aromadendrene	-4.2
44	a-Bisabolol	-2.8
45	a-Elemol	-2.1
46	Caryophyllene oxide	-2.8
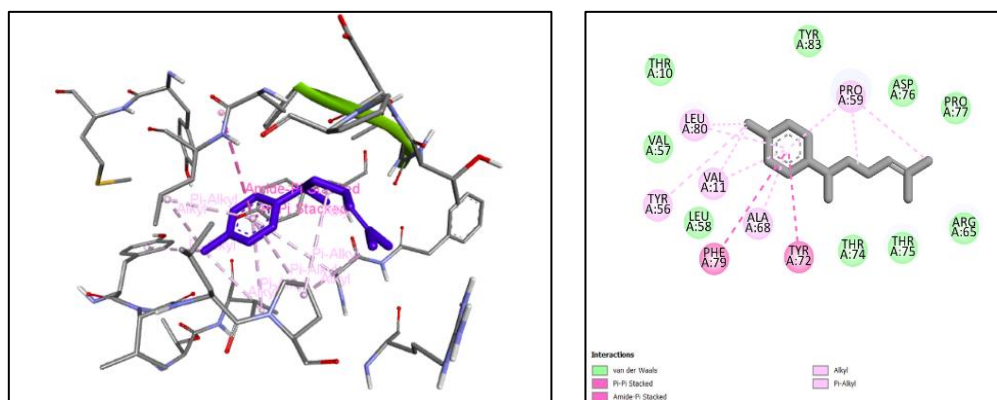
Figure 3. **Visualization of 3D and 2D structures of amino acid residues and the interaction of ar curcumene chemical bonds with 7OFT receptors**

5. Molecular Dynamic Simulation

Based on RMSD and RMSF plot analyses utilizing molecular dynamics simulations, the ar-curcumene and PLpro complexes for SARS-CoV-2 appear to be very stable and have the lowest flexibility compared to HBA as the native ligand and molnupiravir as the reference ligand. (See **Figure 4** and **Figure 5**).
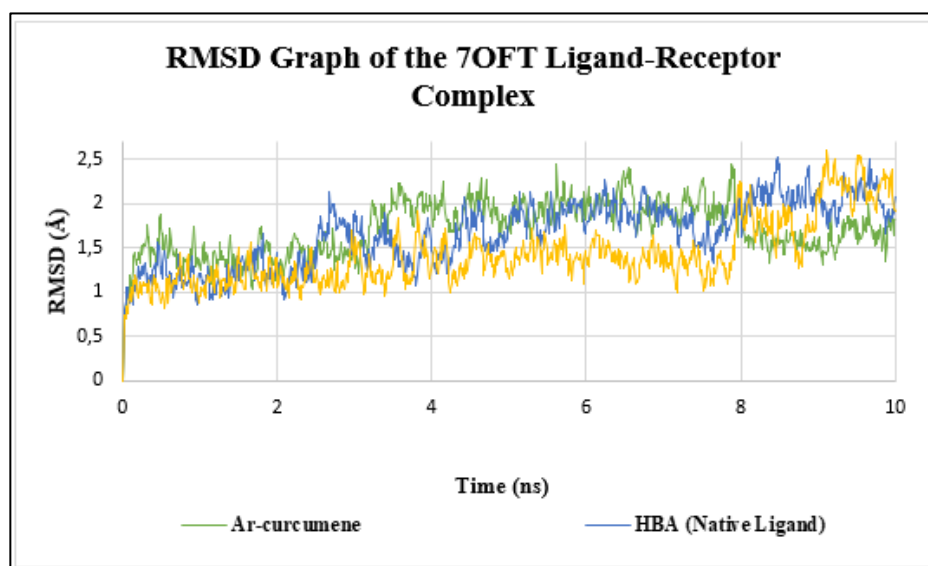
Figure 4. RMSD Graph of the 7OFT Ligand-Receptor Complex
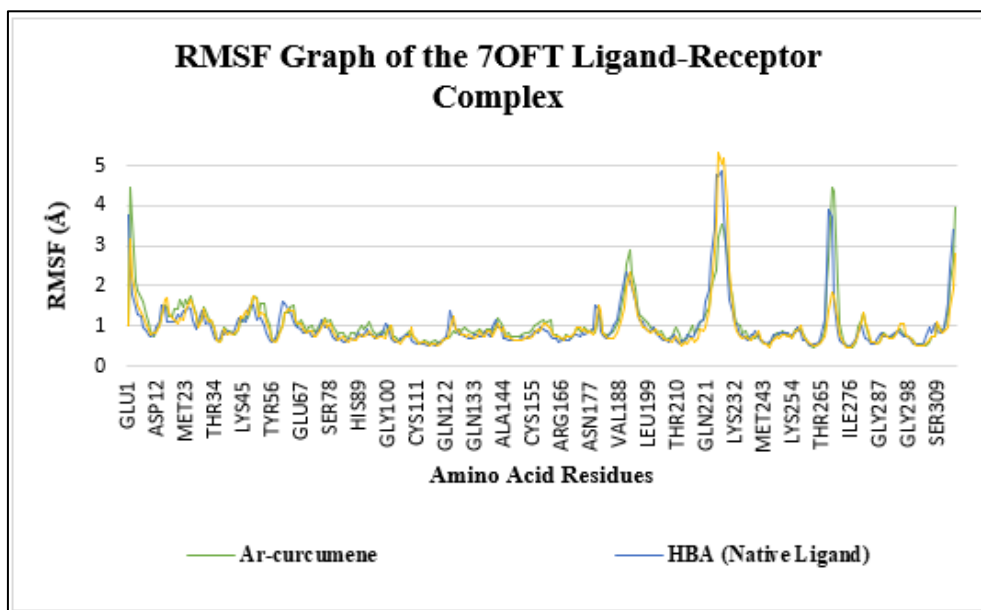
Figure 5. RMSF Graph of the 7OFT Ligand-Receptor Complex

CONCLUSION

In this in silico study, 44 secondary metabolites of red ginger rhizome were examined to identify a lead compound against SARS-CoV-2. Molecular docking results suggest that ar-curcumene is the most promising compound for MD simulation studies. The stable trajectories and low RMSD and RMSF values revealed the structural stability of the ligand-receptor complex. Furthermore, these results were complemented by the pre-ADMET and drug-likeness analyses. Ar-curcumene is potential to be developed as PLpro of SARS-CoV-2 inhibitor. Hence, ar-curcumene could be further developed as a candidate drug for COVID-19 treatment.

ACKNOWLEDGEMENT

REFERENCES

Abdelli, I. *et al.* (2021) 'In silico study the inhibition of angiotensin converting enzyme 2 receptor of COVID-19 by Ammoides verticillata components harvested from Western Algeria', *Journal of Biomolecular Structure and Dynamics*, 39(9), pp. 3263–3276. Available at: https://doi.org/10.1080/07391102.2020.1763199.

Amin, S., Rajabnezhad, S. and Kohli, K. (2009) 'Amin et al.pdf', *Academicjournals.Org*, pp. 1175–1183. Available at: http://www.academicjournals.org/journal/SRE/article-abstract/AA409EC18758.

Assegaf, S., Kawilarang, A.P. and Handajani, R. (2020) 'Antibacterial Activity Test of Red Ginger Extract (Zingiber officinale var. Rubrum) Against Streptococcus pyogenes In vitro', *Biomolecular and Health Science Journal*, 3(1), p. 24. Available at: https://doi.org/10.20473/bhsj.v3i1.19130.

Babadaei, M.M.N. *et al.* (2020) 'Development of remdesivir repositioning as a nucleotide analog against COVID-19 RNA dependent RNA polymerase', *Journal of Biomolecular Structure and Dynamics*, 0(0), pp. 1–9. Available at: https://doi.org/10.1080/07391102.2020.1767210.

Basit, A., Ali, T. and Rehman, S.U. (2021) 'Truncated human angiotensin converting enzyme 2; a potential inhibitor of SARS-CoV-2 spike glycoprotein and potent COVID-

19 therapeutic agent', *Journal of Biomolecular Structure and Dynamics*, 39(10), pp. 3605–3614. Available at: https://doi.org/10.1080/07391102.2020.1768150.

Bhargava, S. *et al.* (2012) 'Zingiber Officinale : Chemical and phytochemical screening and evaluation of its antimicrobial activities', *Journal of Chemical and Pharmaceutical Research*, 4(1), pp. 360–364. Available at: www.jocpr.com.

Cheng, F. *et al.* (2012) 'AdmetSAR: A comprehensive source and free tool for assessment of chemical ADMET properties', *Journal of Chemical Information and Modeling*, 52(11), pp. 3099–3105. Available at: https://doi.org/10.1021/ci300367a.

Eliza Arman (2016) 'Pengembangan Dosis Pemberian Serbuk Kering Jahe Merah (Zingiber officinale var. rubrum) terhadap Pasien Diabetes Mellitus Tipe 2', *Jurnal Medika Saintika*, 7(2), pp. 69–75.

Fikri, F., Saptarini, N.M. and Levita, J. (2016) 'The Inhibitory Activity on the Rate of Prostaglandin Production by Zingiber officinale var. Rubrum', *Pharmacology and Clinical Pharmacy Research*, 1(1). Available at: https://doi.org/10.15416/pcpr.v1i1.15200.

Ghasemzadeh, A., Jaafar, H.Z.E. and Rahmat, A. (2015) 'Optimization protocol for the extraction of 6-gingerol and 6-shogaol from Zingiber officinale var. rubrum Theilade and improving antioxidant and anticancer activity using response surface methodology', *BMC Complementary and Alternative Medicine*, 15(1), pp. 1–10. Available at: https://doi.org/10.1186/s12906-015-0718-0.

Hartati, S., Kebidanan, A. and Negeri, S. (2022) 'Efektifitas Jahe Merah Terhadap Frekuensi Emesis Gravidarum Pada Ibu Hamil Trimester I', *Jurnal Endurance*, 6(3), pp. 468–473. Available at: https://doi.org/10.22216/jen.v6i3.391.

Hasan, A. *et al.* (2021) 'A review on the cleavage priming of the spike protein on coronavirus by angiotensin-converting enzyme-2 and furin', *Journal of Biomolecular Structure and Dynamics*, 39(8), pp. 3025–3033. Available at: https://doi.org/10.1080/07391102.2020.1754293.

Lambrinidis, G., Vallianatou, T. and Tsantili-Kakoulidou, A. (2015) 'In vitro, in silico and integrated strategies for the estimation of plasma protein binding. A review', *Advanced Drug Delivery Reviews*, 86, pp. 27–45. Available at: https://doi.org/10.1016/j.addr.2015.03.011.

Needle, D., Lountos, G.T. and Waugh, D.S. (2015) 'Structures of the Middle East respiratory syndrome coronavirus 3C-like protease reveal insights into substrate specificity', *Acta Crystallographica Section D: Biological Crystallography*, 71, pp. 1102–1111. Available at: https://doi.org/10.1107/S1399004715003521.

Sholikhati, Farikhah and Ridwanto (2022) 'Antioxidant Effect in Red Ginger (Zingiber Officinale Var. Rubrum) Extract during the COVID-19 Pandemic', pp. 1157–1162. Available at: https://doi.org/10.26911/icphmedicine.fp.08.2021.09.

Sinha, S.K. *et al.* (2021) 'An in-silico evaluation of different Saikosaponins for their potency against SARS-CoV-2 using NSP15 and fusion spike glycoprotein as targets', *Journal of Biomolecular Structure and Dynamics*, 39(9), pp. 3244–3255. Available at: https://doi.org/10.1080/07391102.2020.1762741.

Suharyani, I. *et al.* (2021) 'Review Artikel: Potensi Senyawa Aktif Pada Tanaman Obat Untuk Penanganan Covid-19 Dengan Metode Molecular Docking', *Medical Sains : Jurnal Ilmiah Kefarmasian*, 6(2), pp. 115–122. Available at: https://doi.org/10.37874/ms.v6i2.270.